

Distribution Grid Modeling Using Smart Meter Data

Yifei Guo, *Member, IEEE*, Yuxuan Yuan¹, *Graduate Student Member, IEEE*,
and Zhaoyu Wang², *Senior Member, IEEE*

Abstract—The knowledge of distribution grid models, including topologies and line impedances, is essential for grid monitoring, control and protection. However, such information is often unavailable, incomplete or outdated. The increasing deployment of smart meters (SMs) provides a unique opportunity to tackle this issue. This paper proposes a two-stage framework for distribution grid modeling using SM data. In the first stage, the network topology is identified by reconstructing a weighted Laplacian matrix of distribution networks. In the second stage, a least absolute deviations (LAD) regression model is developed for estimating line impedance of a single branch based on the nonlinear (inverse) power flow model, wherein a conductor library is leveraged to narrow down the solution space. The LAD regression model is originally a mixed-integer nonlinear program whose continuous relaxation is still non-convex. Thus, we specially address its convex relaxation and discuss the exactness. The modified regression model is then embedded within a bottom-up sweep algorithm to achieve the identification across the network in a branch-wise manner. Numerical results on the IEEE 13-bus, 37-bus and 69-bus test feeders validate the effectiveness of the proposed methods.

Index Terms—Distribution grid, inverse power flow, line impedance estimation, topology identification, smart meter, convex relaxation.

I. INTRODUCTION

WITH the increasing penetration of distributed energy resources (DERs), grid monitoring and energy management are imperative to distribution system operation [1]. However, such functionalities require complete and accurate knowledge of distribution grid models, including network topologies and line parameters. Unlike transmission systems that enjoy a high level of data redundancy, distribution grid models could be inaccurate or even unavailable [2]. Some utilities only have simple one-line diagrams of their systems without detailed line parameters; other utilities may have system models, but they are often incomplete or outdated due to the frequent system expansion and reconfiguration. Field inspection is a conventional approach to draw the model information, which is laborious, costly, and time-consuming, especially for large-scale systems [3]. This

Manuscript received January 30, 2021; revised June 10, 2021 and August 28, 2021; accepted October 3, 2021. This work was supported in part by National Science Foundation under EPCN 2042314 and in part by Advanced Grid Modeling Program at the U.S. Department of Energy Office of Electricity under Grant DE-OE0000875. Paper no. TPWRS-00165-2021.

The authors are with the Department of Electrical and Computer Engineering, Iowa State University, Ames, IA 50011 USA (e-mail: yifeig@iastate.edu; yuanyx@iastate.edu; wzy@iastate.edu).

Color versions of one or more figures in this article are available at <https://doi.org/10.1109/TPWRS.2021.3118004>.

Digital Object Identifier 10.1109/TPWRS.2021.3118004

suggests an urgent need of efficient and tractable approaches for distribution grid modeling.

In recent years, the deployment of advanced monitoring and metering infrastructures, e.g., smart meters (SMs) and microphasor measurement units (μ PMUs), provides an opportunity to extract the distribution grid models from field measurements [4]. Some studies extend the classical state estimation tools [5]–[8] to infer the status of switches, shunt capacitors/reactors, etc. [9]–[12]. However, this paper considers a different problem: the general distribution grid modeling consisting of a full topology and parameter identification of the whole network from scratch instead of only detecting the status of switchable devices. This cannot be easily handled by generalizing the state estimation tools.

Recently, data-driven approaches for network topology and parameter identification have attracted a lot of attention. These methods can be roughly classified into two categories according to whether they require complex voltage and current measurements (i.e., phase angle information). The studies of the first category rely on high-granularity synchrophasor measurements [13]–[16]. In [13], a multi-run optimization method was proposed to estimate line parameters of a three-phase distribution feeder based on the synchronized voltage phasors and line flow measurements. The authors in [14] proposed to identify network topology based on both fundamental and harmonic synchrophasor data by solving a mixed-integer linear program. With the help of phase angle information, the work of [15] jointly estimates the network topology and parameters by directly reconstructing the admittance matrix. In [16], a similar joint estimation was achieved by carrying out the topology and parameter identification alternately. Note that these phasor-based methods require a high or even full coverage of μ PMUs, which is cost-prohibitive, especially for low-voltage (LV) grids. In addition, the existing joint topology and parameter estimation methods need to solve a large-scale centralized optimization program and may require iterations between topology and parameter identification; thus, the computational complexity significantly grows with the network size.

Rather than using synchrophasor measurements, another line of research managed to identify topology or parameters using voltage magnitude and power measurements [17]–[23]. In [17], a mixed-integer quadratic programming (QP) model was developed to identify network topology with the known line impedance information. In [18], a structure learning method was developed to estimate the grid topology by assuming the nodal power injections are uncorrelated or with non-negative covariances. In [19] and [20], correlation

analysis-based algorithms were proposed to identify the grid topology using SM data, under the assumption that the correlation/similarity between customers' voltage profiles increases as the electrical distance decreases. In [21], a Markov random field-based algorithm was proposed to detect the topology based on uncorrelated power loads. Notice that such statistical assumptions may be challenged by the high penetration of behind-the-meter DERs. The authors in [22] formulated the parameter identification problem as a maximum likelihood estimation model based on the linearized power flow. In [23], an error compensation model was developed to achieve a robust estimation of distribution line parameters.

It is observed that the existing methods in this category either conduct topology identification based on some prior line parameter information (e.g., impedance or R/X ratio), or perform parameter identification with a known topology. A joint network topology and parameter estimation is still challenging in the sense that such prior information is usually unavailable in practice. Statistical methods usually need massive measurement streams, composed of several hours or even many days of recorded data. This may hinder them from detecting topology changes in real time.

In this context, we propose a novel two-stage framework to identify network topology and parameters in this paper. In the first stage, we develop a novel topology identification method, which consists of a linear least squares (LS) model for estimating a weighted Laplacian matrix (WLM) and a density-based clustering method for recovering topology from the estimated WLM. Different with existing methods, the proposed topology identification initially builds on distribution grids with a homogeneous R/X ratio, which yields a tractable fitting model. Then, its robustness against heterogeneous R/X ratios is also analyzed and demonstrated.

In the second stage, a nonlinear least absolute deviations (LAD) regression model is developed for parameter estimation of a single branch based on the branch flow model [24]. To improve the accuracy of parameter estimation, the LAD regression model establishes on the nonlinear power flow, which is therefore nonlinear and nonconvex. Then, we propose a convex relaxation method of the LAD model. A conductor library is exploited to significantly narrow the solution space of parameter estimation. Finally, a bottom-up sweep algorithm is proposed to accomplish the parameter estimation across the entire system by carrying out the estimation of line impedance and line flow, alternatively.

The topology identification solves an unconstrained convex QP program and the density-based clustering method needs to scan the whole network only once. The parameter estimation is performed in a branch-wise manner, so that the computational complexity is approximately *linear* with the network size. Therefore, the proposed method enjoys good computational efficiency and scalability.

The rest of this paper is organized as follows. Section II gives the preliminaries including the power flow model, some facts and basic assumptions, used for developing the proposed method. Sections III and IV present the details of topology identification and line impedance estimation methods, respectively. Numerical

test results are provided in Section V. Some discussions in terms of robustness and scalability is given in Section VI, followed by conclusions.

II. PRELIMINARIES

Regarding notation, for a column vector \mathbf{v} , let v_i denote its i th entry; and $\|\mathbf{v}\|_1$ and $\|\mathbf{v}\|_2$ denote its \mathcal{L}_1 -norm and \mathcal{L}_2 -norm, respectively. Given a matrix \mathbf{M} , let m_{ij} denote its entry at i -th row and j -th column and $[\mathbf{M}]_i$ denotes its i th row; \mathbf{M}^{-1} , \mathbf{M}^T and \mathbf{M}^{-T} denote its inverse, transpose and inverse transpose, respectively. Let $\mathbf{1}_n$ be the $n \times 1$ column vector with all entries being 1 and \mathbf{I}_n be the $n \times n$ identity matrix. The superscript (\bullet) denotes the *estimation* and $(\bullet)^*$ means the *optimum*.

Consider a radial distribution grid comprised of $n + 1$ buses. Let $\mathcal{N} \cup \{0\}$ be the set of buses where the secondary side of substation transformer is indexed by 0 (the unique slack bus in the distribution grid) and $\mathcal{N} := \{1, \dots, n\}$ denotes the set of other buses. For any $j \in \mathcal{N}$, $\mathcal{C}_j \subseteq \mathcal{N}$ denotes its children bus set. \mathcal{P}_j denotes the set of buses in the *unique* path from bus j to bus 0 (including bus j itself). Without loss of generality, we uniquely label a branch by its downstream end bus (i.e., branch j 's downstream end is bus j). In this way, we are able to characterize the network only by bus labels.

The proposed topology and parameter identification methods both build on the branch flow model [24] that relaxes the voltage angle. For notation convenience throughout this paper, we modify the original version by *splitting* the power balance equations as:

$$P_j = \sum_{k \in \mathcal{C}_j} \bar{P}_k - p_j, \quad \bar{P}_j = P_j + r_j \cdot \frac{P_j^2 + Q_j^2}{v_j} \quad (1a)$$

$$Q_j = \sum_{k \in \mathcal{C}_j} \bar{Q}_k - q_j, \quad \bar{Q}_j = Q_j + x_j \cdot \frac{P_j^2 + Q_j^2}{v_j} \quad (1b)$$

$$v_i - v_j = 2(r_j P_j + x_j Q_j) + (r_j^2 + x_j^2) \cdot \frac{P_j^2 + Q_j^2}{v_j} \quad (1c)$$

for any $j \in \mathcal{N}$, where p_j, q_j denote the *net* real/reactive power injection at bus j ; \bar{P}_j, \bar{Q}_j denote the real and reactive power flowing from the upstream bus i ; P_j, Q_j denote the real and reactive power flowing to the downstream bus j ; $r_j, x_j > 0$ are the line resistance and reactance; v_i and v_j are the *squared* voltage magnitude at buses i and j .

Different than the power flow analysis that solves voltages and line flows, the line impedance and topology information will be extracted based on the known voltage and line flows, which is referred to as *inverse power flow* [25].

Some facts and assumptions throughout this paper are clarified as below:

- The proposed method only considers balanced distribution networks. This is due to the invisibility of the grid-edge phase angle information. In this work, the available data source required only consists of voltage magnitude and power measurements recorded by SMs. In practice, this method can be applied for balanced medium-voltage (MV) systems or single-phase LV grids.

- It is assumed that there is a full coverage of SM with nodal net load and voltage magnitude measurements. This assumption is consistent with the recent expansion of smart grid monitoring devices. By the end of 2020, about 107 million SMs had been deployed, covering about 75% of U.S. households [26]. Further, although reactive power measurement is rarely collected in practice, SMs are, in fact, able to measure reactive power in real time. Utilities do not activate this function due to financial and data storage concerns.
- Typically, SMs are installed on the LV customer side. So, SM data should be aggregated if they are used for MV grids. For example, the customer power measurements are aggregated at secondary transformer level.
- The SM data used for identification is assumed to be perfect since data quality problems are not the primary focus of this work. Though this may not be the case in practice, a number of advanced data pre-processing [27]–[30] and pseudo measurement generation methods [31]–[33] can be implemented first to mitigate the impact of and data quality issues (e.g., asynchrony, bad data, missing data).
- A library of line conductor types is assumed to be known, which is typically available in practice, in the sense that the conductor types are often well recorded by utilities.

III. NETWORK TOPOLOGY IDENTIFICATION BASED ON WEIGHTED LAPLACIAN MATRIX

In this section, we firstly develop an optimization-based topology identification method for distribution grids with the homogeneous R/X ratio, and then discuss its robustness against the variability of R/X ratios.

A. Link Between Grid Topology and Power Flow

Assuming the line loss is negligible compared to line flow¹, a linear approximation of (1) that neglects the nonlinear terms in (1) is conducted as,

$$\mathbf{v} \simeq 2\mathbf{A}^{-T}\mathbf{R}\mathbf{A}^{-1}\mathbf{p} + 2\mathbf{A}^{-T}\mathbf{X}\mathbf{A}^{-1}\mathbf{q} - v_0\mathbf{A}^{-T}\mathbf{a}_0 \quad (2)$$

where $\mathbf{v} := [v_1, \dots, v_n]^T$, $\mathbf{p} := [p_1, \dots, p_n]^T$, and $\mathbf{q} := [q_1, \dots, q_n]^T$ denote the vectors collecting squared bus voltage magnitudes, real power and reactive power injections at buses $1, \dots, n$, respectively; $[\mathbf{a}_0, \mathbf{A}^T]^T \in \{0, \pm 1\}^{(n+1) \times n}$ is the incidence matrix of the radial-topology graph where \mathbf{a}_0^T denotes the first row of the incidence matrix; $\mathbf{R} := \text{diag}(r_1, \dots, r_n)$ and $\mathbf{X} := \text{diag}(x_1, \dots, x_n)$ are diagonal matrices with j -th diagonal entry being the resistance and reactance of j -th branch.

Regarding the sort order within \mathbf{p}, \mathbf{q} and \mathbf{v} , it should be clarified that the entries within vectors \mathbf{p}, \mathbf{q} and \mathbf{v} can be sorted without any prior restriction. To be more clear, buses $1, \dots, n$ can be arbitrarily labelled regardless of the actual bus position in the network. The *only* requirement is that they should be organized in a coherent way, meaning p_j, q_j and v_j that characterize bus j should come from the same SM.

¹Since line losses are usually much smaller than power flows, the approximation error is relatively small, typically at the order of 1% [34].

For a radial distribution network, the reduced incidence matrix $\mathbf{A} := [a_{ij}]_{n \times n}$ is non-singular [35] and $\mathbf{A}^{-T}\mathbf{a}_0 = -\mathbf{1}_n$. Therefore, a variant of (2) reads,

$$\frac{1}{2} \underbrace{\mathbf{A}\mathbf{X}^{-1}\mathbf{A}^T}_{\mathbf{Y}}(\mathbf{v} - v_0\mathbf{1}_n) = \underbrace{\mathbf{A}\mathbf{X}^{-1}\mathbf{R}\mathbf{A}^{-1}}_{\mathbf{\Phi}}\mathbf{p} + \mathbf{q} \quad (3)$$

where $\mathbf{Y} := [y_{ij}]_{n \times n}$ is a weighted *Laplacian* matrix of the network with the entries being:

$$y_{ij} = y_{ji} = \begin{cases} -1/x_j, & \text{if } j \in \mathcal{C}_i \\ \sum_{k \in \{j\} \cup \mathcal{C}_j} 1/x_k, & \text{if } i = j \\ 0, & \text{otherwise.} \end{cases} \quad (4)$$

Mathematically, the rationale behind \mathbf{Y} is: for any two distinct buses i and j , $y_{ij} < 0$ if they are (directly) physically connected and otherwise, $y_{ij} = 0$. In a physical sense, \mathbf{Y} is structurally close to the admittance matrix but without considering the line resistance. Therefore, if one can (approximately) identify \mathbf{Y} that uniquely characterizes the connectivity, the topology can be extracted accordingly. This inspires a \mathbf{Y} -based topology identification method.

B. Identification Model

We thus attempt to develop a regression model of \mathbf{Y} based on (3) and the measurements of $\mathbf{p}, \mathbf{q}, \mathbf{v}$ and v_0 that can be obtained from SM data. It minimizes the mismatch between both sides of (3). Unfortunately, $\mathbf{\Phi}$ involves the network topology and parameters that are unknown yet.

But interestingly, suppose the network has a homogeneous R/X ratio, i.e.,

$$\frac{r_1}{x_1} = \dots = \frac{r_n}{x_n} = \lambda, \quad (5)$$

$\mathbf{\Phi}$ reduces to

$$\mathbf{\Phi} = \mathbf{A} \begin{bmatrix} r_1/x_1 & & \\ & \dots & \\ & & r_n/x_n \end{bmatrix} \mathbf{A}^{-1} = \lambda \mathbf{I}_n. \quad (6)$$

Accordingly, (3) becomes,

$$\mathbf{Y}(\mathbf{v} - v_0\mathbf{1}_n) = 2(\lambda\mathbf{p} + \mathbf{q}). \quad (7)$$

This exactly eliminates the requirement of prior information regarding \mathbf{A}, \mathbf{R} and \mathbf{X} , and relies on $\mathbf{p}, \mathbf{q}, \mathbf{v}$ and v_0 .

Then, defining the mismatch vector regarding k -th sample,

$$\mathbf{e}^{(k)} := \widehat{\mathbf{Y}}(\mathbf{v}^{(k)} - v_0^{(k)}\mathbf{1}_n) - 2\lambda\mathbf{p}^{(k)} - 2\mathbf{q}^{(k)}, \quad \forall k \quad (8)$$

and $\mathbf{e} := [(\mathbf{e}^{(1)})^T, \dots, (\mathbf{e}^{(K)})^T]^T$ where $K \gg n$ is the total number of samples, a linear LS regression model of \mathbf{Y} reads,

$$\underset{\widehat{\mathbf{Y}}, \lambda}{\text{minimize}} \|\mathbf{e}\|_2^2. \quad (9)$$

Clearly, this fitting model is an unconstrained convex QP program that can be efficiently solved.

Algorithm 1: Recovering Topology From $\widehat{\mathbf{Y}}$ by Clustering.**Initialization:** Initialize $i \leftarrow 1, j \leftarrow 1, \gamma, \xi$ **repeat**[S1]: Select the i th row of $\widehat{\mathbf{Y}}$.**repeat**[S2]: Pick \widehat{y}_{ij} and retrieve all direct density-reachable points using ξ .[S3]: Based on γ , if \widehat{y}_{ij} is a core point, a cluster is formed; otherwise, update $j \leftarrow j + 1$.**until** $j = n$ or no new point can be added to any cluster[S4]: Update $i \leftarrow i + 1$.**until** $i = n$.

271 C. Recovering Topology From Weighted Laplacian Matrix

272 Recovering the topology from $\widehat{\mathbf{Y}}$ can be cast as an *anomaly*
 273 *detection* problem based on the property in (4). Considering the
 274 sparsity of the distribution grid topology, a density-based spatial
 275 clustering of applications with noise method [36] is utilized here,
 276 which is tabulated as Algorithm 1. The rationale behind our task
 277 is that most of the entries in $\widehat{\mathbf{Y}}_i$ for all i , are concentrated on
 278 a small range, which can be grouped into several clusters that
 279 represent the unconnected buses; the non-diagonal entries that
 280 do not belong to these clusters are declared as anomalies which
 281 indicate the connectivity. To achieve this, the method uses a
 282 minimum density level estimation based on two user-defined
 283 hyperparameters, a threshold for the minimum number of neigh-
 284 bors, γ , and the radius, ξ . \widehat{y}_{ij} with more than γ neighbors within ξ
 285 distance are considered to be a core point. All neighbors within
 286 the ξ radius of a core point are considered to be part of the
 287 same cluster as the core point. Based on multiple core points,
 288 all entries in $\widehat{\mathbf{Y}}$ can be separated by clusters of lower density.
 289 The cluster with the minimum entries is considered to contain
 290 the connected buses. Overall, our method leverages the density
 291 drop between the unconnected and the connected entries in $\widehat{\mathbf{Y}}$
 292 to detect the cluster boundaries for recovering topology from
 293 estimated weighted Laplacian matrix. Unlike other clustering
 294 algorithms that assume normally shaped clusters, this method is
 295 capable of finding clusters with arbitrary shapes and sizes. More-
 296 over, it does not require *a priori* specification on the number of
 297 clusters, therefore ensuring the robustness and practicality [37].
 298 Note that it does not enforce radiality.

299 D. Robustness Analysis on Heterogeneous Networks

300 As mentioned above, the proposed regression model is derived
 301 on the assumption of a homogeneous R/X ratio, which may
 302 not be true in practical networks. However, a distribution grid
 303 at a given voltage level has the *relatively heterogeneous* R/X
 304 ratios [38], which is widely believed to hold in many practical
 305 cases (see [39] for some examples). In what follows, we will
 306 show that our proposed method has some robustness against the
 307 heterogeneous R/X ratios.

308 Let $\bar{\lambda} := (\lambda_1 + \dots + \lambda_n)/n$ be the mean of R/X ratios and
 309 accordingly, let $\lambda_j := \bar{\lambda} + \Delta\lambda_j, \forall j$, where $\Delta\lambda_j$ denotes the

deviation to λ . Therefore, we have,

$$\Phi = \bar{\lambda}\mathbf{I}_n + \Delta\lambda \quad (10)$$

where $\Delta\lambda := \mathbf{A}\text{diag}(\Delta\lambda_1, \dots, \Delta\lambda_n)\mathbf{A}^{-1}$.

311 *Proposition 1:* Matrix $\Delta\lambda := [\Delta\lambda_{ij}]_{n \times n}$ is a matrix with the
 312 entries being,
 313

$$\Delta\lambda_{ij} = \begin{cases} \Delta\lambda_i - \Delta\lambda_{C_i \cap P_j}, & \text{if } i \in P_j \\ \Delta\lambda_i, & \text{if } i = j \\ 0, & \text{otherwise.} \end{cases} \quad (11)$$

314 The proof is provided in the appendix. Observe (11), $\Delta\lambda$ can
 315 be used to quantify the heterogeneity of R/X across the whole
 316 network. For a network with relatively homogeneous R/X ratios,
 317 $\lambda_j \simeq \bar{\lambda}, \forall j$ and consequently, $|\Delta\lambda_i| \simeq 0$ and $|\Delta\lambda_i - \Delta\lambda_j| \simeq$
 318 $0, \forall i, j$. Therefore, $\Delta\lambda$ will not significantly affect the solution
 319 of (9) provided the program is numerically stable. And for a
 320 strictly homogeneous network, (10) completely reduces to (6).

IV. LINE IMPEDANCE ESTIMATION: LAD REGRESSION MODEL AND BOTTOM-UP SWEEP FRAMEWORK

321 Here, we develop a regression model for line impedance
 322 estimation of a *single* branch—a LAD model with mixed-integer
 323 semidefinite programming (MISDP) formulation. It is then em-
 324 bedded with a *bottom-up* sweep algorithm to accomplish the
 325 parameter estimation across the entire network.
 326

327 Keep in mind that the proposed regression model is built on
 328 full nonlinear inverse power flow instead of its linearized coun-
 329 terpart, in the sense that the latter may be unable to accurately
 330 recover the parameters, especially when the regression problem
 331 is ill-posed [40]; see Fig. 1 for a numerical example on the IEEE
 332 13-bus feeder. Note that, the non-convexity of the nonlinear in-
 333 verse power flow model makes the regression problems NP-hard
 334 even after continuous relaxation. This motivates us to specially
 335 address its convexification.
 336

A. Regression Model for a Single Branch

337 The line impedance estimation establishes on the voltage drop
 338 relationship (1 e). Define the vector of model mismatch $\mathbf{e}_j :=$
 339 $[e_j^{(1)}, \dots, e_j^{(K)}]^T$ for all $j \in \mathcal{N}$ with
 340

$$e_j^{(k)} := v_i^{(k)} - v_j^{(k)} - 2 \left(\widehat{r}_j P_j^{(k)} + \widehat{x}_j Q_j^{(k)} \right) - \left(\widehat{R}_j + \widehat{X}_j \right) \cdot \frac{\left(P_j^{(k)} \right)^2 + \left(Q_j^{(k)} \right)^2}{v_j^{(k)}}, \forall k \quad (12)$$

341 where x_j and r_j denote the estimation of r_j and x_j ; $\widehat{R}_j := \widehat{r}_j^2$
 342 and $\widehat{X}_j := \widehat{x}_j^2$.

343 The impedance estimation minimizes the \mathcal{L}_1 -norm (LAD) of
 344 \mathbf{e}_j , which is expected to hold the following features. On the
 345 one hand, the nonlinearity of the inverse power flow is well-
 346 captured to guarantee estimation accuracy. On the other hand, the
 347 library of R/X ratios (obtained from the line conductor library) is
 348 exploited to significantly narrow the solution space; otherwise,
 349 the solution may easily fall into some remote local optimum.
 350 Therefore, the line impedance estimation, which is inherently

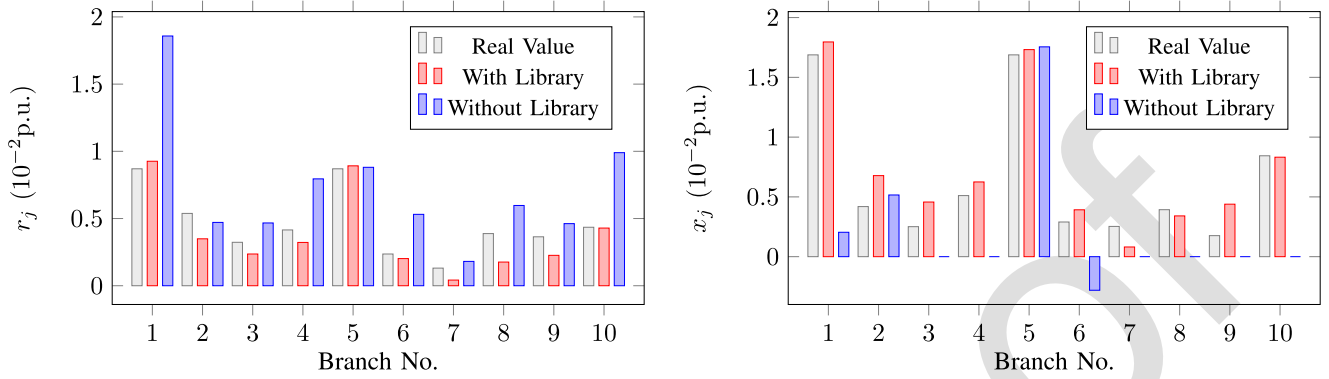


Fig. 1. Least-squares-based line parameter estimation results of the modified IEEE 13-bus test feeder (see Section V for details) based on the linearized inverse power flow model with and without the help of a R/X ratio library.

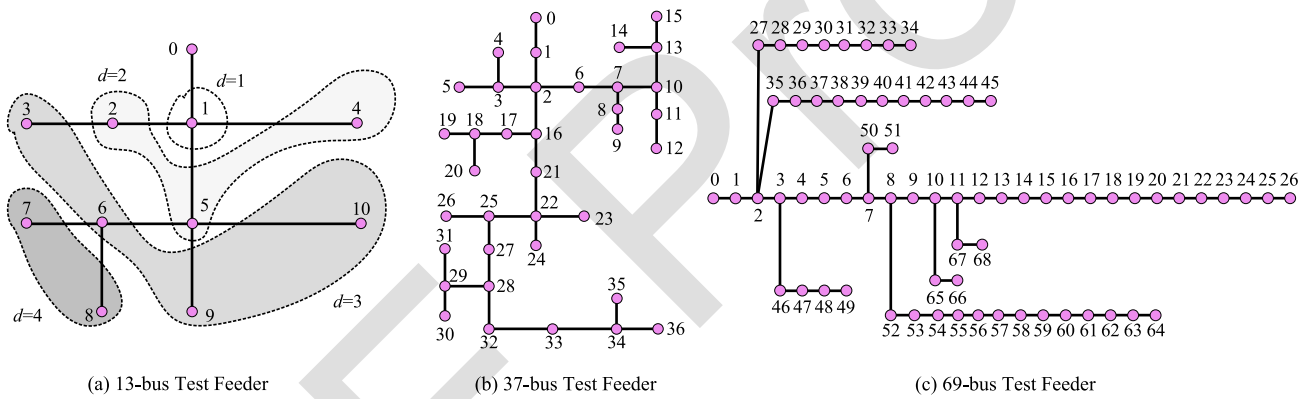


Fig. 2. One-line diagrams of the modified IEEE (a) 13-bus, (b) 37-bus and (c) 69-bus test feeders (balanced) where the original 13-bus test feeder is modified to a 11-bus test feeder by removing the dummy buses 634 and 692 of the original case and the line impedance of 69-bus feeder are slightly modified to achieve several typical R/X ratios. The resultant R/X ratio libraries are $\{0.5153, 1.2840, 0.8124, 0.8112, 0.9864, 2.0655\}$, $\{1.4536, 1.6222, 2.7482, 1.9691\}$, and $\{0.4000, 0.8000, 0.9000, 2.0000, 2.9000, 3.0000, 3.1000, 3.3000, 3.4000\}$ in the three cases, respectively.

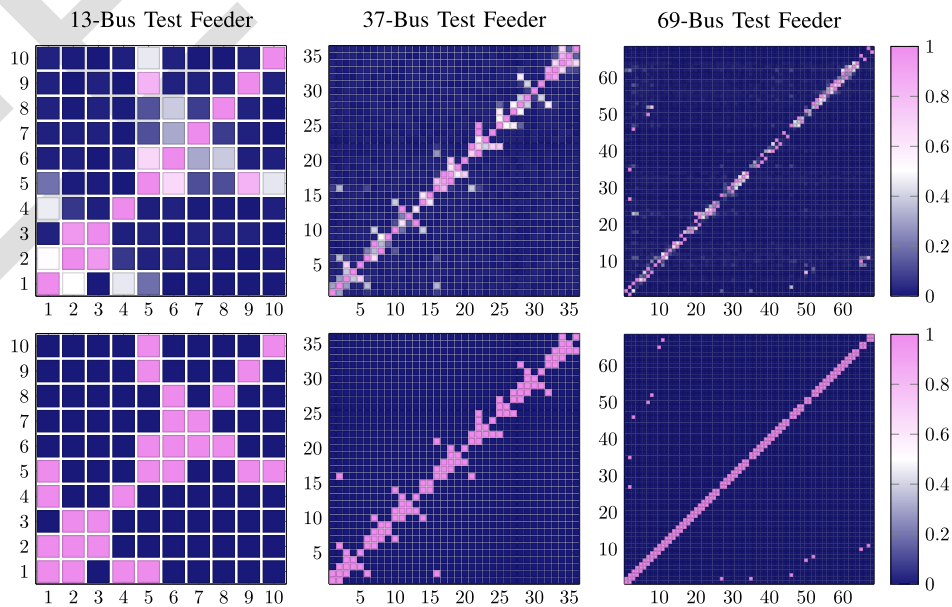


Fig. 3. Results of topology identification of the modified IEEE 13-bus (left), 37-bus (middle), and 69-bus (right) test feeders. The top part shows the normalized counterpart of \hat{Y} . The bottom part shows the output of Algorithm 1, which represents the connectivity.



Fig. 4. Results of line parameter estimation of 13-, 37- and 69-bus test feeders.

351 a combinatorial optimization problem, can be cast as a mixed-
 352 integer nonlinear programming (MINLP) model by introducing
 353 the binary variables $\alpha_1, \dots, \alpha_H$,

$$\underset{\alpha_h, r_j, x_j, R_j, X_j}{\text{minimize}} \quad f(\mathbf{e}_j) := \|\mathbf{e}_j\|_1 \quad (13a)$$

$$\text{subject to} \quad \widehat{R}_j = \widehat{r}_j^2 \quad (13b)$$

$$\widehat{X}_j = \widehat{x}_j^2 \quad (13c)$$

$$\widehat{r}_j = \sum_{h=1}^H \lambda_h \alpha_h \widehat{x}_j \quad (13d)$$

$$\sum_{h=1}^H \alpha_h = 1, \alpha_h \in \{0, 1\}, \forall h. \quad (13e)$$

The Big-M technique is exploited to linearize the bilinear term $\alpha_h x_j$ as,

$$-M_j(1 - \alpha_h) \leq \widehat{r}_j - \lambda_h \widehat{x}_j \leq M_j(1 - \alpha_h), \forall z \quad (14)$$

where M_j is a large real number. 356

While (13) can be handled by some general MINLP solvers, 357
 there is no guarantee of global optimality since its continuous 358
 relaxation counterpart is still non-convex due to the quadratic 359

360 constraints (13 b) and (13 c). Therefore, in what follows, we
361 will discuss the convexification.

362 To make the optimization model tractable, we first rewrite the
363 cost function in an equivalent form without \mathcal{L}_1 -norm operator
364 by introducing the auxiliary variables $\theta_j^{(1)}, \dots, \theta_j^{(K)}$:

$$f(\theta_j^{(1)}, \dots, \theta_j^{(K)}) = \sum_{k=1}^K \theta_j^{(k)} \quad (15)$$

365 with the additional constraints,

$$\theta_j^{(k)} \geq e_j^{(k)}, \quad -\theta_j^{(k)} \leq e_j^{(k)}, \quad \forall k. \quad (16)$$

366 To tackle the non-convex quadratic equalities (13 b) and (13
367 c), we propose to convexify them via SDP relaxation. We first
368 rewrite (13 b) and (13 c) as,

$$\mathbf{W}_j^r := \begin{bmatrix} 1 & \hat{r}_j \\ \hat{r}_j & \hat{R}_j \end{bmatrix} \succeq 0, \quad \text{rank} \{ \mathbf{W}_j^r \} = 1, \quad \forall j \quad (17a)$$

$$\mathbf{W}_j^x := \begin{bmatrix} 1 & \hat{x}_j \\ \hat{x}_j & \hat{X}_j \end{bmatrix} \succeq 0, \quad \text{rank} \{ \mathbf{W}_j^x \} = 1, \quad \forall j. \quad (17b)$$

369 Then, removing the rank-1 constraints in (17), a MISDP model
370 whose continuous relaxation is a convex SDP, is given by,

$$\text{minimize}_{\alpha_n, r_j, x_j, R_j, X_j, \theta_j^{(k)}} \sum_{k=1}^K \theta_j^{(k)} \quad (18a)$$

$$\text{subject to} \quad \theta_j^{(k)} \geq e_j^{(k)}, \quad \forall k \quad (18b)$$

$$-\theta_j^{(k)} \leq e_j^{(k)}, \quad \forall k \quad (18c)$$

$$\mathbf{W}_j^r \succeq 0 \quad (18d)$$

$$\mathbf{W}_j^x \succeq 0 \quad (18e)$$

$$(13e) \text{ and } (14). \quad (18f)$$

371 In this way, it can be handled by MISDP solvers. The follow-
372 ing proposition provides a sufficient condition that guarantees
373 the SDP relaxation is exact while the estimation is error-free.

374 *Proposition 2:* Let $\mu := [r_j, x_j, r_j^2, x_j^2]^T$. If μ is the optimal
375 solution of (18), then the SDP relaxation is exact and the esti-
376 mation is exact.

377 The proof is provided in the appendix. Proposition 2 implies
378 that if the measurements are error-free, such sufficient condition
379 naturally holds because $f(\mu) = \inf f = 0$. If the measurements
380 are erroneous but the errors do not affect the optimal solution
381 (i.e., such sufficient condition still holds), the relaxation is still
382 exact. Furthermore, if the errors are so large that the resultant
383 optimal solution of (18) is no longer equal to μ , it is still possible
384 that such relaxation is exact but it depends on the properties of
385 samples.

386 B. Bottom-Up Sweep Algorithm

387 Clearly, developing (18) requires the knowledge of voltage
388 magnitude and line flow values. Unfortunately, due to the low
389 coverage of line flow sensors, there are few line flow measure-
390 ments available. Exceptions are the *tail* branches since they have

Algorithm 2: Bottom-Up Sweep Algorithm.

Initialization: Initialize $d \leftarrow D$.

repeat

[S1]: Update the $P_j^{(k)}$ and $Q_j^{(k)}$ by (1 a) and (1 b) for all
 $k = 1, \dots, K$ and j in layer d .

[S2]: Calculate r_j, x_j of each line segment by solving
(18) for all j in layer d .

[S3]: Calculate $\bar{P}_j^{(k)}$ and $\bar{Q}_j^{(k)}$ as per (1 c) and (1 d) for
all $k = 1, \dots, K$ and j in layer d .

[S4]: Update $d \leftarrow d - 1$.

until $d = 0$.

no further downstream neighbors, and thus the line flows phys- 391
ically equal the power injections at the leaf buses, which can be 392
measured by SMs. Moreover, as per (1 a)–(1 b), *the line flow over* 393
a given branch can be calculated, provided all of its neighboring 394
downstream line flows have been known. These facts motivate 395
the design of a bottom-up (a.k.a. leaf-to-root) sweep algorithm 396
that manipulates the line flow and line impedance estimation in 397
an alternating way. 398

We first partition a radial distribution network into multiple 399
layers which are labeled as $1, \dots, D$ where D is the maximum 400
depth [see Fig. 2(a) for an example with $D = 4$]. Physically, 401
bus j belongs to layer d means there are d intermediate line 402
segments in the path from bus j to the root bus 0. As stated in 403
Section II, for a radial network, there is a unique path from any 404
bus j to the root bus 0. Therefore, the partition of layers is unique 405
as well. The bottom-up sweep algorithm with the breadth-first 406
search is tabulated as Algorithm 2. 407

V. NUMERICAL RESULTS 408

In this section, the proposed topology and parameter identi- 409
fication methods are verified on the modified IEEE 13, 37 410
and 69-bus test feeders, which are depicted in Fig. 2. We have 411
utilized the real SM data from our utility partners in Midwest 412
to replace the load data of these benchmark systems. More 413
precisely, the available customer power measurements with 1-h 414
resolution are aggregated at secondary transformer level by 415
summing them at different times. The power flow analysis takes 416
as input these distribution system models and the nodal load 417
demand time-series. The computed nodal voltages are treated 418
as the voltage measurements, along with the load time-series, 419
used for topology and parameter identification. In this work, 420
the length of the time window is 200 samples. Following the 421
previous works [37], the minimum number of neighbors, γ , 422
and the radius ξ in topology recovery are assigned as 2 and 3, 423
respectively. The optimization programs are solved by YALMIP 424
Toolbox in MATLAB, along with the solver MOSEK [41]. 425

A. Results of Topology Identification 426

The topology identification results of the modified IEEE 13- 427
bus, 37-bus and 69-bus test feeders are depicted in Fig. 3. For 428
data visualization, the min-max normalization [42] is utilized to 429
rescale the entries of $[\hat{\mathbf{Y}}]_i$ to be within $[0, 1]$ for all i . 430

431 The upper part of Fig. 3 illustrates the *rescaled* variant of
 432 matrices $\hat{\mathbf{Y}}$ of each test feeder. Then, by performing Algorithm
 433 1, the estimated connectivity between any two buses of each
 434 test feeder is obtained (see the bottom part of Fig. 3 where
 435 “0” denotes “unconnected” and “1” denotes “connected”). The
 436 performance is validated by comparing the estimated connect-
 437 ivity and the real connectivity. In this work, the proposed
 438 method achieves a 100% accurate topology recovery for all the
 439 three distribution feeders. Note that, this verifies our method’s
 440 robustness against heterogeneous R/X ratios.

441 B. Results of Line Parameter Estimation

442 The line parameter estimation results of the modified IEEE
 443 13-bus, 37-bus and 69-bus test feeders are depicted in Fig. 4. As
 444 can be seen from Fig. 4, the SDP-based LAD model precisely
 445 recovers the line impedance of each branch, under all the three
 446 test cases. In terms of r_j , the largest relative errors (among all
 447 branches) are $3.33 \times 10^{-5}\%$, $3.40 \times 10^{-4}\%$ and $1.44 \times 10^{-4}\%$
 448 for the modified IEEE 13-bus, 37-bus and 69-bus test feeders,
 449 respectively; and as for x_j , the largest relative errors are $3.33 \times$
 450 $10^{-5}\%$, $3.40 \times 10^{-4}\%$ and $7.06 \times 10^{-5}\%$, respectively.

451 To quantify the exactness of SDP relaxation in (18), that is
 452 how close are the matrices \mathbf{W}_j^r and \mathbf{W}_j^x to rank one, one can
 453 compute the ratio between their largest two eigenvalues, i.e.,
 454 $\sigma_2(\mathbf{W})/\sigma_1(\mathbf{W})$. The maximum values of $\sigma_2(\mathbf{W}^r)/\sigma_1(\mathbf{W}^r)$
 455 among all branches are 6.77×10^{-11} , 6.33×10^{-10} and $1.49 \times$
 456 10^{-10} for the 13-bus, 37-bus and 69-bus test feeders; and the
 457 maximum values of $\sigma_2(\mathbf{W}^x)/\sigma_1(\mathbf{W}^x)$ among all branches are
 458 6.20×10^{-11} , 9.44×10^{-10} and 1.47×10^{-10} , respectively. It
 459 is demonstrated that the SDP relaxation is exact.

460 VI. DISCUSSIONS

461 A. Robustness

462 For topology identification, given that the nonlinearity of
 463 power flow is dropped in the regression model, it is unlikely
 464 to solve $\hat{\mathbf{Y}}$ to be exactly equal to the true \mathbf{Y} . Yet, in fact, it does
 465 *not* require an exact estimation, because the topology is only
 466 sensitive to the structural feature of the matrix rather than its
 467 exact value. Such a feature makes the proposed method robust
 468 against imperfect data to a certain extent.

469 For line parameter estimation, on the one hand, the conductor
 470 library can reduce the solution space. This may enhance the
 471 numerical stability of the regression model, and reduces the
 472 impact of data quality issues. On the other hand, the proposed
 473 bottom-up sweep algorithm is inherently robust because the
 474 estimation errors regarding downstream branches only affect
 475 the line losses, which slightly contributes to the upstream-end
 476 line flows. It is therefore expected that the effects of estimation
 477 errors can asymptotically diminish.

478 B. Efficiency and Scalability

479 Besides the tractable fitting model of \mathbf{Y} , the density-based
 480 clustering method used for extracting topology from $\hat{\mathbf{Y}}$ is also
 481 efficient since this method scans the whole dataset only one time.
 482 Further, we have applied an indexing structure that executes

a neighboring query in $O(\log n)$. Consequently, the computa-
 483 tional complexity of this anomaly detection is $O(n \log n)$ [37].
 484 In our tests, recovering the topology from the estimated weighted
 485 Laplacian matrix can be done in a few seconds.
 486

The line impedance estimation method has good scalability.
 487 Via SDP relaxation, the LAD regression model (18) can be
 488 easily handled by off-the-shelf solvers (solved in milliseconds
 489 in our tests). The optimization model is designed and solved
 490 in a branch-wise manner whose computation burden does not
 491 grow with network size [the computation burden of (18) is
 492 only related to the number of samples and the size of library].
 493 Besides, the sweep algorithm only requires very simple algebraic
 494 operations for line flow computation, which scales well with the
 495 network size as well. Therefore, the total computation burden for
 496 parameter estimation is approximately linear with the network
 497 size.
 498

The high computational efficiency and good scalability enable
 499 a real-time application of the proposed method after some
 500 system changes (e.g., network reconfiguration).
 501

502 VII. CONCLUSION

In this paper, we propose a data-driven framework to accurately
 503 and efficiently find the connectivity of different nodes in
 504 entire or partial networks using SM data. The proposed topology
 505 identification establishes on reconstructing the weighted
 506 Laplacian matrix of a homogeneous distribution circuit, which
 507 also exhibits provable robustness against heterogeneous R/X
 508 ratios. The mixed-integer nonlinear LAD regression model for
 509 parameter identification is developed and convexified. We then
 510 embed it in a bottom-up sweep algorithm to achieve the line
 511 parameter estimation across the whole network. The test results
 512 validate the effectiveness and accuracy of the proposed methods.
 513

At present, this work only focuses on balanced radial distribution
 514 grids. In future studies, the proposed method will
 515 be generalized to unbalanced and/or meshed grids, with the
 516 help of limited available μ PMU data on a few critical nodes.
 517 Moreover, the proposed method will be enhanced for better
 518 robustness against heterogeneous R/X ratios and various data
 519 quality problems.
 520

521 APPENDIX

522 A. Proof of Proposition 1

Let $\mathbf{B} := \mathbf{A}^{-1}$. First, as per the linear algebra theory, $\mathbf{I}_n \rightarrow \mathbf{B}$
 523 can be accomplished via the elementary row operations, by
 524 which, in turn, one can exactly achieve $\mathbf{A} \rightarrow \mathbf{I}_n$. Second, given
 525 that \mathbf{A} is the reduced incidence matrix of a tree-topology network,
 526 we have $a_{ij} = -1$ if $i = j$, $a_{ij} = 1$ if $i \in \mathcal{P}_j \setminus \{j\}$ and
 527 otherwise, $a_{ij} = 0$. To achieve $\mathbf{A} \rightarrow \mathbf{I}_n$, one has to add the rows
 528 j for all $j \in \{j | i \in \mathcal{P}_j\}$ onto the row i , and then multiply row i
 529 by -1 . Accordingly, one can obtain $\mathbf{B} := [b_{ij}]_{n \times n}$ with
 530

$$b_{ij} = \begin{cases} -1, & \text{if } i \in \mathcal{P}_j \text{ or } i = j \\ 0, & \text{otherwise.} \end{cases} \quad (19)$$

531 And then, we have

$$a_{ik} \cdot b_{kj} = \begin{cases} 1, & \text{if } k \in \{i\} \cap \mathcal{P}_j \\ -1, & \text{if } k \in \mathcal{C}_i \cap \mathcal{P}_j \\ 0, & \text{otherwise} \end{cases} \quad (20)$$

532 which indicates it is non-zero if and only if $i \in \mathcal{P}_j$. Therefore,

$$\begin{aligned} \delta_{ij} &= \mathbf{A}_i \text{diag}(\Delta\lambda_1, \dots, \Delta\lambda_n) \mathbf{B}^j = \sum_{k=1}^n a_{ik} \Delta\lambda_k b_{kj} \\ &= \begin{cases} \Delta\lambda_i - \Delta\lambda_{\mathcal{C}_i \cap \mathcal{P}_j}, & \text{if } i \in \mathcal{P}_j \setminus \{j\} \\ \Delta\lambda_i, & \text{if } i = j \\ 0, & \text{otherwise} \end{cases} \end{aligned} \quad (21)$$

533 for any $i, j \in \mathcal{N}$. ■

534 B. Proof of Proposition 2

535 Let f_{NLP}^* and f_{SDP}^* be the optimal cost function value of (13)
536 and (18). Obviously, it follows that $f_{\text{NLP}}^* \geq f_{\text{SDP}}^*$.

537 It is observed that μ is a feasible solution of (13). If $f_{\text{SDP}}^* =$
538 $f(\mu)$ holds, we have

$$f(\mu) \geq f_{\text{NLP}}^* \geq f_{\text{SDP}}^* = f(\mu). \quad (22)$$

539 This yields $f_{\text{NLP}}^* = f_{\text{SDP}}^* = f(\mu)$, and therefore, the relaxation
540 is exact while the estimation is exact. ■

541 REFERENCES

- 542 [1] K. Dehghanpour, Z. Wang, J. Wang, Y. Yuan, and F. Bu, "A survey on
543 state estimation techniques and challenges in smart distribution systems,"
544 *IEEE Trans. Smart Grid*, vol. 10, no. 2, pp. 2312–2322, Mar. 2019.
- 545 [2] Y. Wang, Q. Chen, T. Hong, and C. Kang, "Review of smart meter
546 data analytics: Applications, methodologies, and challenges," *IEEE Trans.*
547 *Smart Grid*, vol. 10, no. 3, pp. 3125–3148, May 2019.
- 548 [3] F. C. L. Trindade, W. Freitas, and J. C. M. Vieira, "Fault location in
549 distribution systems based on smart feeder meters," *IEEE Trans. Power*
550 *Del.*, vol. 29, no. 1, pp. 251–260, Feb. 2014.
- 551 [4] *Energy Information Administration. Advanced Metering Count by Tech-*
552 *nology Type*. 2017. [Online]. Available: [https://www.eia.gov/electricity/](https://www.eia.gov/electricity/annual/html/epa_10_10.html)
553 [annual/html/epa_10_10.html](https://www.eia.gov/electricity/annual/html/epa_10_10.html)
- 554 [5] A. Primadianto and C.-N. Lu, "A review on distribution system state
555 estimation," *IEEE Trans. Power Syst.*, vol. 32, no. 5, pp. 3875–3883,
556 Sep. 2017.
- 557 [6] K. Dehghanpour, Z. Wang, J. Wang, Y. Yuan, and F. Bu, "A survey on
558 state estimation techniques and challenges in smart distribution systems,"
559 *IEEE Trans. Smart Grid*, vol. 10, no. 2, pp. 2312–2322, Mar. 2019.
- 560 [7] T. Ramachandran, A. Reiman, S. P. Nandanoori, M. Rice, and S. Kundu,
561 "Distribution system state estimation in the presence of high solar pen-
562 etration," in *Proc. Amer. Control Conf.*, 2019, pp. 3432–3437.
- 563 [8] Y. Zhang, A. Bernstein, A. Schmitt, and R. Yang, "State estimation
564 in low-observable distribution systems using matrix completion," *National*
565 *Renewable Energy Lab. (NREL), Golden, CO, USA, Tech. Rep.*,
566 2019.
- 567 [9] F. Wu and W.-H. Liu, "Detection of topology errors by state estimation
568 (power systems)," *IEEE Trans. Power Syst.*, vol. 4, no. 1, pp. 176–183,
569 Feb. 1989.
- 570 [10] G. Korres and P. Katsikas, "Identification of circuit breaker statuses in
571 wls state estimator," *IEEE Trans. Power Syst.*, vol. 17, no. 3, pp. 818–825,
572 Aug. 2002.
- 573 [11] V. Kekatos and G. B. Giannakis, "Joint power system state estimation and
574 breaker status identification," in *Proc. North Amer. Power Symp.*, 2012,
575 pp. 1–6.
- 576 [12] Y. Gao, Z. Zhang, W. Wu, and H. Liang, "A method for the topology
577 identification of distribution system," in *IEEE Power Energy Soc. Gen.*
578 *Meeting*, 2013, pp. 1–5.
- 579 [13] B. Das, "Estimation of parameters of a three-phase distribution feeder,"
580 *IEEE Trans. Power Del.*, vol. 26, no. 4, pp. 2267–2276, Oct. 2011.
- [14] L. Chen, M. Farajollahi, M. Ghamkhari, W. Zhao, S. Huang, and H. Mohsenian-Rad, "Switch status identification in distribution networks using harmonic synchrophasor measurements," *IEEE Trans. Smart Grid*, vol. 12, no. 3, pp. 2413–2424, May 2021.
- [15] J. Yu, Y. Weng, and R. Rajagopal, "PaToPa: A data-driven parameter and topology joint estimation framework in distribution grids," *IEEE Trans. Power Syst.*, vol. 33, no. 4, pp. 4335–4347, Jul. 2018.
- [16] O. Ardakanian *et al.*, "On identification of distribution grids," *IEEE Trans. Control Netw. Syst.*, vol. 6, no. 3, pp. 950–960, Sep. 2019.
- [17] Z. Tian, W. Wu, and B. Zhang, "A mixed integer quadratic programming model for topology identification in distribution network," *IEEE Trans. Power Syst.*, vol. 31, no. 1, pp. 823–824, Jan. 2016.
- [18] D. Deka, S. Backhaus, and M. Chertkov, "Structure learning in power distribution networks," *IEEE Trans. Control Netw. Syst.*, vol. 5, no. 3, pp. 1061–1074, Sep. 2018.
- [19] W. Luan, J. Peng, M. Maras, J. Lo, and B. Harapnuk, "Smart meter data analytics for distribution network connectivity verification," *IEEE Trans. Smart Grid*, vol. 6, no. 4, pp. 1964–1971, Jul. 2015.
- [20] M. Zhang, W. Luan, S. Guo, and P. Wang, "Topology identification method of distribution network based on smart meter measurements," in *Proc. China Int. Conf. Electricity Distrib.*, 2018, pp. 372–376.
- [21] S. Bolognani, N. Bof, D. Michelotti, R. Muraro, and L. Schenato, "Identification of power distribution network topology via voltage correlation analysis," in *Proc. 52nd IEEE Conf. Decis. Control*, 2013, pp. 1659–1664.
- [22] W. Wang and N. Yu, "Parameter estimation in three-phase power distribution networks using smart meter data," in *Proc. Int. Conf. Probabilistic Methods Appl. Power Syst.*, 2020, pp. 1–6.
- [23] A. M. Prostejovsky, O. Gehrke, A. M. Kosek, T. Strasser, and H. W. Bindner, "Distribution line parameter estimation under consideration of measurement tolerances," *IEEE Trans. Ind. Inform.*, vol. 12, no. 2, pp. 726–735, 2016.
- [24] M. E. Baran and F. F. Wu, "Optimal capacitor placement on radial distribution systems," *IEEE Trans. Power Del.*, vol. 4, no. 1, pp. 725–734, Jan. 1989.
- [25] Y. Yuan, S. Low, O. Ardakanian, and C. Tomlin. *Inverse Power Flow Problem*. 2020. [Online]. Available: <https://arxiv.org/abs/1610.06631>
- [26] Institute for Electric Innovation, "Electric company smart meter deployments: Foundation for a smart grid (2021 update)," Apr. 2021.
- [27] Y. Yuan, K. Dehghanpour, and Z. Wang, "Mitigating smart meter asynchrony error via multi-objective low rank matrix recovery," 2021, *arXiv:2105.05175*.
- [28] S. Bolognani, R. Carli, and M. Todescato, "State estimation in power distribution networks with poorly synchronized measurements," in *Proc. 53rd IEEE Conf. Decis. Control*, 2015, pp. 2579–2584.
- [29] A. Alimardani, F. Therrien, D. Atanackovic, J. Jatskevich, and E. Vaahedi, "Distribution system state estimation based on nonsynchronized smart meters," *IEEE Trans. Smart Grid*, vol. 6, no. 6, pp. 2919–2928, Jun. 2015.
- [30] F. Ni, P. H. Nguyen, J. F. Cobben, H. E. van den Brom, and D. Zhao, "Uncertainty analysis of aggregated smart meter data for state estimation," in *IEEE Int. Workshop Appl. Meas. Power Syst.*, 2016, pp. 1–6.
- [31] Y. Yuan, K. Dehghanpour, F. Bu, and Z. Wang, "A multi-timescale data-driven approach to enhance distribution system observability," *IEEE Trans. Power Syst.*, vol. 34, no. 4, pp. 3168–3177, Jul. 2019.
- [32] Y. R. Gahrooei, A. Khodabakhshian, and R. A. Hooshmand, "A new pseudo load profile determination approach in low voltage distribution networks," *IEEE Trans. Power Syst.*, vol. 33, no. 1, pp. 463–472, Jan. 2018.
- [33] D. T. Nguyen, "Modeling load uncertainty in distribution network monitoring," *IEEE Trans. Power Syst.*, vol. 30, no. 5, pp. 2321–2328, Sep. 2015.
- [34] H. Zhu and H. J. Liu, "Fast local voltage control under limited reactive power: Optimality and stability analysis," *IEEE Trans. Power Syst.*, vol. 31, no. 5, pp. 3794–3803, Sep. 2016.
- [35] R. B. Bapat, *Graphs and Matrices*. Berlin, Germany: Springer, 2010.
- [36] E. Schubert, J. Sander, M. Ester, H. P. Kriegel, and X. Xu, "DBSCAN revisited, revisited: Why and how you should (still) use DBSCAN," *ACM Trans. Database Syst.*, vol. 42, no. 3, pp. 1–21, 2017.
- [37] J. Shen, X. Hao, Z. Liang, Y. Liu, W. Wang, and L. Shao, "Real-time superpixel segmentation by DBSCAN clustering algorithm," *IEEE Trans. Image Process.*, vol. 25, no. 12, pp. 5933–5942, Dec. 2016.
- [38] S. Bolognani, R. Carli, G. Cavraro, and S. Zampieri, "Distributed reactive power feedback control for voltage regulation and loss minimization," *IEEE Trans. Autom. Control*, vol. 60, no. 4, pp. 966–981, Apr. 2015.
- [39] W. Kersting, "Radial distribution test feeders," in *Proc. IEEE Power Eng. Soc. Winter Meeting. Conf. Proc.*, 2001, vol. 2, pp. 908–912.

- 656 [40] J. Yang, N. Zhang, C. Kang, and Q. Xia, "A state-independent linear power
657 flow model with accurate estimation of voltage magnitude," *IEEE Trans.*
658 *Power Syst.*, vol. 32, no. 5, pp. 3607–3617, Sep. 2017.
- 659 [41] J. Löfberg, "YALMIP: A toolbox for modeling and optimization in
660 MATLAB," in *Proc. CACSD Conf.*, 2004, pp. 284–289.
- 661 [42] I. Goodfellow, Y. Bengio, and A. Courville, *Deep Learning*. Cam-
662 bridge, MA, USA: MIT Press, 2016. [Online]. Available: [http://www.
663 deeplearningbook.org](http://www.deeplearningbook.org).

664
665
666
667
668
669
670
671
672
673
674
675



Yifei Guo (Member, IEEE) received the B.E. and Ph.D. degrees in electrical engineering from Shandong University, Jinan, China, in 2014 and 2019, respectively. He is currently a Postdoctoral Research Associate with the Department of Electrical and Computer Engineering, Iowa State University, Ames, IA, USA. During 2017–2018, he was a Visiting Student with the Department of Electrical Engineering, Technical University of Denmark, Lyngby, Denmark.

His research interests include distribution system modeling, optimization, and control.

676
677
678
679
680
681
682
683



Yuxuan Yuan (Graduate Student Member, IEEE) received the B.S. degree in 2017 in electrical & computer engineering from Iowa State University, Ames, IA, USA, where he is currently working toward the Ph.D. degree. His research interests include distribution system state estimation, synthetic networks, data analytics, and machine learning.



Zhaoyu Wang (Senior Member, IEEE) received the B.S. and M.S. degrees in electrical engineering from Shanghai Jiao Tong University, Shanghai, China, and the M.S. and Ph.D. degrees in electrical and computer engineering from the Georgia Institute of Technology, Atlanta, GA, USA. He is currently the Northrop Grumman Endowed Associate Professor with Iowa State University. His research interests include optimization and data analytics in power distribution systems and microgrids. He was the recipient of the National Science Foundation CAREER Award, the

Society-Level Outstanding Young Engineer Award from IEEE Power and Energy Society (PES), the Northrop Grumman Endowment, College of Engineering's Early Achievement in Research Award, and the Harpole-Pentair Young Faculty Award Endowment. He is the Principal Investigator for a multitude of projects funded by the National Science Foundation, the Department of Energy, National Laboratories, PSERC, and Iowa Economic Development Authority. He is the Chair of IEEE PES PSOPE Award Subcommittee, the Co-Vice Chair of PES Distribution System Operation and Planning Subcommittee, and the Vice Chair of PES Task Force on Advances in Natural Disaster Mitigation Methods. He is an Associate Editor for the *IEEE TRANSACTIONS ON POWER SYSTEMS*, *IEEE TRANSACTIONS ON SMART GRID*, *IEEE OPEN ACCESS JOURNAL OF POWER AND ENERGY*, *IEEE POWER ENGINEERING LETTERS*, and *IET Smart Grid*.

684
685
686
687
688
689
690
691
692
693
694
695
696
697
698
699
700
701
702
703
704
705
706
707
708